

## Robust optimization of a hybrid control system for wind-exposed tall buildings with uncertain mass distribution

Ilaria Venanzi\* and Annibale Luigi Materazzi

*Department of Civil and Environmental Engineering University of Perugia, Perugia, Italy*

*(Received January 28, 2013, Revised March 10, 2013, Accepted May 30, 2013)*

**Abstract.** In this paper is studied the influence of the uncertain mass distribution over the floors on the choice of the optimal parameters of a hybrid control system for tall buildings subjected to wind load. In particular, an optimization procedure is developed for the robust design of a hybrid control system that is based on an enhanced Monte Carlo simulation technique and the genetic algorithm. The large computational effort inherent in the use of a MC-based procedure is reduced by the employment of the Latin Hypercube Sampling. With reference to a tall building modeled as a multi degrees of freedom system, several numerical analyses are carried out varying the parameters influencing the floors' masses, like the coefficient of variation of the distribution and the correlation between the floors' masses. The procedure allows to obtain optimal designs of the control system that are robust with respect to the uncertainties on the distribution of the dead and live loads.

**Keywords:** robust optimization; Monte Carlo simulation; latin hypercube sampling; active tuned mass dampers; tall buildings; wind load

---

### 1. Introduction

To mitigate the wind-induced response of high-rise buildings several types of control devices can be used that provide the building with additional damping, increasing the performance of the structure (Casati *et al.* 2012).

Among the control systems, hybrid control devices such as Active Tuned Mass Dampers (ATMDs), are particularly effective as they need a lower actuation power with respect to the purely active systems and can work as passive devices when power supply is missing. Another advantage of the hybrid control is that, unlike the purely passive system, it can adjust to the load uncertainties and to the variations of the system dynamic characteristics, at the price of an increase in the performance demand of the system. In a general framework of limited resources and system constraints on control forces, damping and strokes, it is important to perform a robust design optimization to obtain a controlled system almost independent on the variations of the external conditions.

In the technical literature many analytical and numerical methods were proposed for the choice of the optimal parameters of passive and hybrid systems under different types of excitation

---

\*Corresponding author, Assistant Professor, E-mail: [ilaria.venanzi@strutture.unipg.it](mailto:ilaria.venanzi@strutture.unipg.it)

(Warburton 1982, Hoang *et al.* 2008). More recently, robust optimization methods started to be discussed accounting for the uncertainties on the dynamic characteristics of the structure and/or the external loading (Chen *et al.* 2007, Moreno and Thomson 2010, Chakraborty and Roy 2011).

The robust optimization is the process of finding a design solution that is relatively invariant with respect to uncertain parameters changes. This goal is opposite to the target of the optimization because the best solution in general is not the most robust one (Beyer and Sendhoff 2007). The target pursued by the designers is to provide a high degree of robustness even at the expense of the system's performance. The structural robustness is assessed by the measure of the performance variability around the expected value. The task of reducing the scatter of the structural performance without eliminating the source of variability is the target of the robust design (Doltsinis and Kang 2004).

Among the robust optimization methods, those treating the uncertainties directly within the optimization problem are referred to as simulation optimization (Schueller and Jensen 2008). These problems are usually solved by direct optimization methods that do not require an estimate of the gradients of the functions. In order to perform robust optimization, the robustness measures like expectancy and dispersion measures (expected values and variances), must be calculated from the information obtained by simulation (Lee and Park 2001, Jensen 2006). The most well-known simulation technique is the Monte Carlo method (MC) whose main limitation is the requirement of a significant computational effort. Among the enhanced simulation methods, the

Importance Sampling (IS) (Zhang 2012, Grooteman 2011) the Latin Hypercube Sampling (LHS) (Huntington and Lyrantzis 1998, Olsson *et al.* 2003), the Line Sampling (LS) (Pradlwarter *et al.* 2007, Katafygiotis and Wang 2009) and the Subset Simulation (SS) (Li and Au 2010, Song *et al.* 2009) are available tools for an efficient estimation of the robustness.

Uncertainties in structural dynamics may be stochastic, like seismic (Marano and Greco 2009) and wind loads (Cluni *et al.* 2007) or epistemic, related to the lack of information that could be reduced by additional information (Pascual and Adhikari). Although the uncertainties on the mass and the stiffness of the structural system (or on the natural frequency that accounts for both mass and stiffness uncertainty) were often considered in the optimal design of control systems (Marano *et al.* 2010), the topic of the uncertain mass distribution over the height of the building and over the floors' surface was not deeply investigated. As the loads vary from floor to floor and over the floors' surface, there is significant variability on the mass distribution corresponding especially to the live loads variations. The design of the control system is usually carried out considering an uniformly distributed mass corresponding to the design value of the dead and live loads which can be significantly different from the actual mass distribution. Because of this discrepancy, the natural frequencies and the modal masses that are used for the optimization of the control system can be significantly different and therefore the control system can be less effective.

In this paper the influence of the uncertain mass distribution over the floors on the robust design of the optimal parameters of a hybrid control system for tall buildings subjected to wind load is studied. The design of the parameters is carried out using an optimization procedure based on an enhanced Monte Carlo simulation of the uncertain parameters distribution and a genetic algorithm. In particular, an optimization of the design parameters of the control system is carried out for each sample mass matrix allowing the evaluation of the probability distribution of the optimal parameters. The large computational effort required by the Monte Carlo method is reduced by the use of the Latin Hypercube Sampling, a stratified random procedure that provides an efficient way of simulating variables from their multivariate distributions, taking samples from equally probable intervals. The robust optimization procedure is applied to a tall building modeled

as a multi degrees of freedom system and subjected to wind loads obtained from wind tunnel tests. Several optimizations are carried out varying the parameters which influence the distribution of the floors' masses, like the coefficient of variation and the correlation of the distribution over the floors. The robust designs are selected to have corresponding values of the objective function lying in the neighborhood of the expected value.

## 2. Dynamics of the controlled system

The hybrid control system considered in this paper, is capable to control the translational and torsional response of the structure. It can be schematized with  $n$  ATMDs located at the top floor of a tall building (Venanzi *et al.* 2013).

The structure is schematized considering 3 DOFs for each floor. The total number of DOFs of the system is  $3p + p'$ , where  $p$  is the total number of storeys and  $p'$  is the number of DOFs of the ATMDs. Assuming that the aeroelastic effects are negligible, hypothesis that is acceptable for low wind speed in service conditions (Venanzi and Materazzi 2012), the classical equation of motion for the controlled system is

$$\mathbf{M}_s \ddot{\mathbf{q}} + \mathbf{C}_s \dot{\mathbf{q}} + \mathbf{K}_s \mathbf{q} = \mathbf{f} + \mathbf{B}_0 \mathbf{u} \quad (1)$$

where  $\mathbf{q}$  is the vector of the generalized displacements,  $\mathbf{M}_s$ ,  $\mathbf{C}_s$  and  $\mathbf{K}_s$  are the mass, damping and stiffness matrices, respectively,  $\mathbf{f}$  is the vector of the wind loads,  $\mathbf{u}$  is the vector of the control forces and  $\mathbf{B}_0$  is a location matrix. The damping matrix is computed according to the classical Rayleigh model  $\mathbf{C}_s = \alpha \mathbf{M}_s + \beta \mathbf{K}_s$ , where  $\alpha$  and  $\beta$  are functions of the circular frequencies and the damping ratio.

The state space formulation of the equation of motion of the controlled system obtained by Eq. (1) is

$$\dot{\mathbf{z}} = \mathbf{A} \mathbf{z} + \mathbf{B} \mathbf{u} + \mathbf{H} \mathbf{f} \quad (2)$$

where  $\mathbf{Z} = [\mathbf{q} \dot{\mathbf{q}}]^T$  is the state vector,  $\mathbf{A}$  is the system matrix,  $\mathbf{B}$  and  $\mathbf{H}$  are the location matrices for the vectors  $\mathbf{u}$  e  $\mathbf{f}$ , respectively.

Owing to the common availability of accelerometers as monitoring sensors, tracking of the state using only acceleration measurements is here considered. In particular, three accelerometers per floor are used to measure the alongwind, acrosswind and torsional accelerations.

The output,  $\mathbf{y}$ , thus results in a linear combination of generalized nodal accelerations, as

$$\mathbf{y} = \mathbf{C}_a \ddot{\mathbf{q}} \quad (3)$$

where  $\mathbf{C}_a$  is a convenient matrix that selects the monitored DOFs.

Eq. (3) can be rewritten in terms of state vector and control forces as

$$\mathbf{y} = \mathbf{C} \mathbf{z} + \mathbf{D} \mathbf{u} + \mathbf{H} \mathbf{f} + \mathbf{v} \quad (4)$$

where

$$\begin{aligned} \mathbf{C} &= -\mathbf{C}_a \begin{bmatrix} \mathbf{M}_s^{-1} \mathbf{K}_s & \mathbf{M}_s^{-1} \mathbf{C}_s \end{bmatrix} \\ \mathbf{D} &= \mathbf{C}_a \mathbf{M}_s^{-1} \mathbf{B}_0 \end{aligned} \quad (5)$$

and  $\mathbf{v}$  is the vector of measurement noise.

Without loss of generality, the linear optimal control algorithm is used for the problem at hand. The linear quadratic performance index can be written as

$$J = \frac{1}{2} \int_0^{\infty} (\mathbf{z}^T \mathbf{Q} \mathbf{z} + \mathbf{u}^T \mathbf{R} \mathbf{u}) dt \quad (6)$$

where  $\mathbf{Q}$  and  $\mathbf{R}$  are the weighting matrices of the state vector and the control forces vector respectively. By application of the classic LQR algorithm the optimal gain matrix  $\mathbf{K}$ , which allows minimizing the performance index  $J$ , is computed and the feedback is calculated as  $\mathbf{u} = -\mathbf{K} \mathbf{z}$ .

### 3. Uncertain mass modeling

The uncertainty on the mass distribution leads to the uncertainty on the natural frequencies of the structure that affects the optimal design of the control system. The uncertain mass can be modeled as follows:

1. the mass is random and doesn't vary from floor to floor. In this case the mass distribution is described by a unique random variable;
2. the mass is random and varies from floor to floor. In this case the mass distribution is described by a set of random variables;
3. the mass is random and varies from floor to floor and over the floors' surface. The mass distribution is described by a three-dimensional random field.

Without loss of generality, in this paper only the uncertainty on the distribution with the height (case 2) is considered, neglecting the spatial variability over the floors.

The mass matrix of the structure  $\mathbf{M}$  has dimensions  $3p \times 3p$  and its terms are the floors' masses  $m_j$  ( $j = 1, \dots, 3p$ ) that are the sums of the masses corresponding to the dead and live loads

$$m_j = \bar{m}_{dj} + \bar{m}_{lj} \pm \Delta m_j = \bar{m}_j \pm \Delta m_j \quad (7)$$

In Eq. (7),  $\bar{m}_{dj}$  is the mean value of the mass corresponding to the dead load,  $\bar{m}_{lj}$  is the mean value of the mass corresponding to the live load,  $\bar{m}_j = \bar{m}_{dj} + \bar{m}_{lj}$  is the mean value of the mass and  $\Delta m_j$  is the random part of the mass. Only the masses corresponding to the translational degrees of freedom  $m_j$  ( $j = 1, \dots, p$ ) are considered as random variables, while the corresponding translational masses in the orthogonal direction and the mass moments of inertia  $m_j$  ( $j = p+1, \dots, 3p$ ) are set correspondingly, considering an uniform mass distribution over the floors. The probability distribution of the random variables representing the floors' masses  $m_j$  must be chosen. For example, a multivariate normal distribution can be selected. It is described by the mean values of the random variables  $\bar{m}_j$ , their standard deviations  $\sigma_j$  and the covariances between the random variables  $\sigma_{hk}$  ( $h, k = 1, \dots, p$ ). The covariances are defined as

$$\sigma_{hk} = \rho \cdot \sigma_h \cdot \sigma_k \quad (8)$$

where  $\rho$  is the correlation coefficient,  $\sigma_h$  and  $\sigma_k$  are the standard deviations of the random variables  $m_h$  and  $m_k$ . The standard deviation is defined as follows

$$\sigma_j = \bar{m}_j \cdot CV \quad (9)$$

#### 4. Robust optimization of the control system

A general robust optimization task can be stated by the following mathematical problem

$$\begin{aligned} & \text{Min } F(\mathbf{y}) \\ & \text{subject to } g_s(\mathbf{y}, \theta) \leq 0 \quad i = 1, \dots, S \\ & \quad \quad \quad s_r(\mathbf{y}, \theta) = 0 \quad j = 1, \dots, R \\ & \quad \quad \quad h_l(\mathbf{y}) \leq 0 \quad l = 1, \dots, L \end{aligned} \quad (10)$$

where  $\mathbf{y}$  is the vector of the design variables,  $\theta$  is the vector of the uncertain parameters,  $F$  is the objective function,  $g_s$  and  $s_r$  are functions that define the set of inequality and equality constraints and  $h_l$  are the functions that define the set of deterministic constraints.

The proposed optimization procedure is aimed at designing a hybrid control system that leads to the maximum response reduction and is robust with respect to the uncertainties on the mass distribution. The method can also take into account the technological limitations of the devices.

The first step of the robust optimization procedure is the application of an enhanced Monte Carlo procedure for the simulation of a large number  $N$  of structural lumped mass matrices  $\mathbf{M}_i$  ( $i = 1, \dots, N$ ) whose diagonal terms  $m_j^i$  ( $j = 1, \dots, p$ ) follow a certain multivariate probability distribution. Solving the eigenvalue problems, the corresponding sets of natural frequencies of the structure  $\Xi_i = [\xi_1^i, \dots, \xi_{3p}^i]$  are computed. The mass-dependent damping matrices are evaluated according to the Rayleigh model using the circular frequencies computed in correspondence of each sample mass matrix.

Then, the optimal design of the hybrid control system is carried out. This consists of a preliminary optimization of the tuning parameters of the control devices considered as purely passive systems and then in the optimization of the parameters that define the LQR performance index. The preliminary optimization of the passive control system, allows increasing the performance of the hybrid control system in terms of power saving. Moreover, if the tuning parameters of the passive devices are optimized independently from the parameters defining the active control algorithm, it is possible to have a control system that works at its best also in case of lack of power supply.

To perform a robust optimization, the mass matrices  $\mathbf{M}_i$  and the sets of natural frequencies  $\Xi_i$  are used as input data for  $N$  optimizations to compute the probability distributions of the objective function and the optimal parameters. From the PDF of the objective function, the robust solutions are identified that are those lying in the neighborhood of the expected value.

##### 4.1 Enhanced Monte Carlo simulation

For the simulation of the uncertain mass matrices of the system an enhanced Monte Carlo method is used.

In order to reduce the high computational effort inherent in the use of a crude Monte Carlo simulation technique, the Latin Hypercube Sampling is adopted. The Latin Hypercube Sampling

(Iman 2008) is a type of enhanced Monte Carlo simulation that provides an efficient way of sampling variables from their multivariate distributions. Let  $N$  denote the number of realizations and  $p$  the number of random variables  $[m_1, m_2, \dots, m_p]$ . The sample space is then  $p$ -dimensional. To generate  $N$  samples from  $p$  variables with probability density function  $f(m)$ , the procedure is as follows. The range of each variable is subdivided into  $N$  non overlapping intervals of equal probability  $1/N$ . From each interval one value is selected at random according to the probability density of the interval. In particular, each value is obtained from the inverse cumulative distribution function as follows

$$m_{j,i} = F_j^{-1} \left( \frac{i-0.5}{N} \right) \quad (11)$$

where  $m_{j,i}$  is the  $i$ -th sample of the  $j$ -th random variable  $m_j$ ,  $F_j^{-1}$  is the inverse cumulative distribution of the variable  $m_j$ . The  $N$  values of the first random variable ( $m_1$ ) are paired in a random manner with the values of the second random variable ( $m_2$ ), these pairs are then paired similarly with the values of  $m_3$  and so on, until  $N$  samples of  $p$  variables are formed. The  $N$   $p$ -dimensional vectors are the Latin Hypercube sample. The pairing is done by associating a permutation of the first  $N$  integers with each input variable in order to match the target correlations.

#### 4.2 Optimization of the passive control system

For each trial value of the mass matrix  $\mathbf{M}_i$ , the parameters of the TMDs are optimized to minimize the response of the controlled modes. In the case of systems with uncertain parameters, like the one considered in this case, the optimal stiffnesses and dampings of the TMDs are random variables. The optimization procedure is aimed at computing the probability distributions of the optimal parameters and therefore at identifying the robust designs.

The total mass of the TMDs,  $m_{TMD_s}$ , is set equal to a conveniently small percentage of the first modal mass of the building  $M_1^*$ ,  $\mu = m_{TMD_s} / M_1^*$  where  $\mu$  is the total mass ratio of the TMDs.

The *design variables* of the optimization procedure are the stiffnesses and the dampings of the TMDs. In particular, the vector of the design variables is

$$\Psi = \{k_1, \dots, k_{p'}, c_1, \dots, c_{p'}\} \quad (12)$$

where  $p'$  is the number of DOFs of the TMDs,  $k_1, \dots, k_{p'}$  are the stiffnesses of the TMDs,  $c_1, \dots, c_{p'}$  are the dampings of the TMDs.

The *objective function* of this optimization problem  $F_1(\Psi)$  is

$$F_1(\Psi) = G_1(\Psi) + P_1(\Psi) = \sum_{h=x,y,\theta} \left\{ \frac{\sigma[q_h(\Psi)]|_{passive}}{\sigma(q_h)|_{uncontrolled}} \right\} + P_1(\Psi) \quad (13)$$

where the first term  $G_1(\Psi)$  is the sum of the ratios between the standard deviations of the generalized displacements  $q_h(\Psi)$ ,  $h = x, y, \theta$  at the top of the building in the case of passively controlled structure  $\sigma[q_h(\Psi)]|_{passive}$  and the standard deviations of the generalized displacements

at the top of the building in the case of uncontrolled structure  $\sigma(q_h)|_{uncontrolled}$ .

The non-linear constraints to the problem are  $\psi_{m,min} \leq \psi_m \leq \psi_{m,max}$ , where  $\psi_m$  is the  $m$ -th term of the design variable vector  $\boldsymbol{\psi} (m=1, \dots, 2p')$  and  $\psi_{m,min}$  and  $\psi_{m,max}$  are the lower and upper bounds of the terms of the design variable vector that depend on the technical characteristics of the selected control devices. To keep into account the constraints, a suitable penalty function  $p_1(\boldsymbol{\psi})$  is added to the objective function when the constraints are violated in order to discard the solution.

To solve the proposed optimization problem, one of the evolutionary algorithms like the genetic algorithm (Goldberg 1989), the simulated annealing algorithm (Venanzi and Materazzi 2007), the direct search algorithm (Conn and Le Digabel 2013) can be used as they do not require knowing the gradient of the objective function. In this paper, the genetic algorithm is adopted that is based on the natural selection, the process that drives biological evolution (Casciati 2008). It repeatedly modifies a population of individual solutions selecting at each step individuals at random from the current population to be parents and using them to produce, through selection, crossover and mutation, the children for the next generation.

#### 4.3 Optimization of the hybrid control system

For each trial value of the mass matrix, the optimal choice of the weight matrices  $\mathbf{R}$  and  $\mathbf{Q}$  of the control force and state vectors in the LQR performance index (Eq. (6)) is obtained through an optimization procedure.

The matrix  $\mathbf{R}$  that weights the control forces is defined as follows

$$\mathbf{R} = 10^{-\varphi_1} \cdot \mathbf{I}_1 \tag{14}$$

where  $\varphi_1$  is a coefficient and  $\mathbf{I}_1$  is an identity matrix.

The matrix  $\mathbf{Q}$  is the product between an identity matrix  $\mathbf{I}_2$  and a diagonal matrix that stores a set of coefficients  $\varphi_2, \dots, \varphi_n$

$$\mathbf{Q} = \begin{bmatrix} \varphi_2 & \dots & 0 \\ \dots & \dots & \dots \\ 0 & \dots & \varphi_n \end{bmatrix} \cdot \mathbf{I}_2 \tag{15}$$

The components of the vector

$$\boldsymbol{\Phi} = [\varphi_1, \dots, \varphi_n]^T \tag{16}$$

are the design variables of this second optimization problem.

The objective function  $F_2(\boldsymbol{\Phi})$ , is defined as follows

$$F_2(\boldsymbol{\Phi}) = G_2(\boldsymbol{\Phi}) + P_2(\boldsymbol{\Phi}) = \sum_{h=x,y,\theta} \left\{ \frac{\sigma[q_h(\boldsymbol{\Phi})]_{hybrid}}{\sigma(q_h)|_{passive}} \right\} + P_2(\boldsymbol{\Phi}) \tag{17}$$

where  $G_2(\boldsymbol{\Phi})$  is the sum of the ratios between the standard deviations of the generalized displacements at the top of the building in the case of hybridly controlled structure

$\sigma[q_h(\Phi)]_{\text{hybrid}}$  and the standard deviations of the generalized displacements at the top of the building in the case of passively controlled structure  $\sigma(q_h)|_{\text{passive}}$  while  $P_2(\Phi)$  is a penalty function.

Some *constraints* can be applied to the design variables

$$\varphi_{v,\min} \leq \varphi_v \leq \varphi_{v,\max} \quad v = 1, \dots, n \quad (18)$$

where the limits  $\varphi_{v,\min}$  and  $\varphi_{v,\max}$  are assigned on the basis of a preliminary sensitivity analysis.

Additional *constraints* can be applied on the maximum control forces and strokes of the ATMDs

$$\begin{cases} u_t \leq u_{\max} \\ q_{ATMD,t} \leq q_{ATMD,\max} \end{cases} \quad (t = 1, \dots, p') \quad (19)$$

where  $u_t$  is the  $t$ -th term of the control force,  $u_{\max}$  is the upper bound of the control force,  $q_{ATMD,t}$  is the  $t$ -th stroke of the ATMDs,  $q_{ATMD,\max}$  is the upper bound to the stroke of the ATMDs. The limits depend on the technological characteristics of the selected control devices. To solve this second optimization problem the genetic algorithm is used.

## 5. Numerical analyses

### 5.1 Description of the case study

The optimization procedure is applied to a prismatic tall building 180 m high with side lengths  $A = 60$  m,  $B = 30$  m. The 60-storeys structure is made of steel with central cores and systems of bracings in both the principal directions. Floors are reinforced concrete slabs capable of warranting a rigid in-plane behavior. A finite element model of the structure is built and used for the preliminary sizing of the structural elements. Then, for the robust optimization procedure, the structure is modeled as a simplified dynamic system having 6 nodes, equally spaced every 10 floors. Each node has 3 DOFs and the stiffness matrix of the system is obtained by static condensation from the finite element model of the structure.

Without loss of generality, a simplified control system made of 3 unidirectional ATMDs is considered: the central ATMD is located at the elastic center of the top floor of the building and is expected to control the alongwind response and the 2 lateral ATMDs are located symmetrically in eccentric position ( $C = 20$  m,  $D = 5$  m, Fig. 1) and are expected to control the torsional response. The total mass ratio of the control system is  $\mu = 2\%$  of the first mode mass of the building. The mass ratio of the central ATMD is  $\mu_c = 1.5\%$  while the total mass ratio of the lateral ATMDs is  $\mu_l = 0.5\%$ .

### 5.2 Wind load modeling

The forcing functions representing the wind load were obtained from synchronous pressure measurements carried out in the wind tunnel (Venanzi and Materazzi 2012, Gioffrè *et al.* 2004). Experimental tests were carried out in the boundary-layer wind tunnel operated by CRIACIV

(Inter-university Research Center on Buildings Aerodynamic and Wind Engineering) in Prato, Italy.

The rigid 1/500 scale model of the building was instrumented with 120 pressure taps, 30 for each side. The sampling frequency was 250 Hz and the duration of the records 30 s. Tests were carried out with a wind speed profile and turbulence intensity corresponding to open terrain conditions. In particular, the exponent of the mean wind profile was 0.17, the mean wind speed at the top of the model was  $V_m = 18.3$  m/s and the turbulence intensity at the same height was the 6%.

It was chosen to neglect the similitude on the Reynolds number because for prismatic structures its effect on the estimation of the pressure coefficients is negligible. Therefore, for the prototype building it was arbitrarily chosen to use a 10-minute average reference wind speed at 10 meters above the ground  $V_r = 30$  m/s. According to the logarithmic law proposed by the Eurocode 1, it corresponds in open terrain (Terrain category II) to a mean wind speed at the top  $V_p = 46.7$  m/s.

In this study, the wind is considered acting in direction  $x$  (Fig. 1).

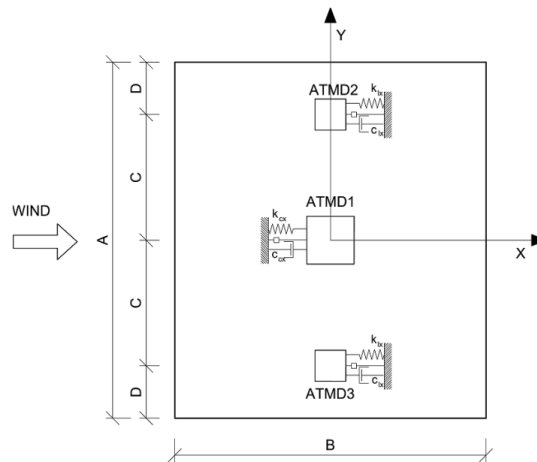


Fig. 1 Plan view of the control system

### 5.3 Probabilistic distribution of the natural frequencies

In order to evaluate the robust optimal parameters of the control system, the preliminary step is to generate a large number of random mass matrices of the system using the Latin Hypercube Sampling.

The mean value of the mass corresponding to the dead load varies from floor to floor while the mean value of the mass corresponding to the live load is  $\bar{m}_1 = 130 \text{ kg/m}^2$ . This value corresponds to a design value of the live load of about  $\bar{m}_1^{des} = 200 \text{ kg/m}^2$ , if the 95<sup>th</sup> percentile of the normal distribution and a coefficient of variation  $CV = 0.3$  is adopted.

The samples generation is carried out considering a multivariate normal distribution of the floors' masses with three different values of the correlation coefficient  $\rho = 0$ ,  $\rho = 0.5$ ,  $\rho = 1$  and three different values of the coefficient of variation  $CV = 0.2$ ,  $CV = 0.4$ ,  $CV = 0.6$ . The maximum

coefficient of variation of  $CV = 0.6$  is chosen in order to have the mass corresponding to the live load varying in the range  $[0 - 260 \text{ kg/m}^2]$  if the confidence level corresponding to the 90% probability is considered.

To avoid the possibility of having non positive definite mass matrices, a preliminary check allows to identify and discard the unfeasible sample mass matrices. In correspondence of each random mass matrix, the natural frequencies of the system are computed through modal analysis.

A preliminary sensitivity analysis allowed to set the number  $N$  of random samples that are required for the correct estimation of the mean values and the standard deviations of the first 3 natural frequencies of the system. In particular, assuming as target values those obtained with a standard Monte Carlo (MC) simulation with  $N=10000$  samples, the Latin Hypercube Sampling (LHS) with  $N=500$  samples leads to sufficiently precise results (Table 1).

Table 1 Sensitivity analysis on the number of random samples ( $\rho = 0.5$  and  $CV = 0.4$ )

		SMC N=10000	LHS N=10000	LHS N=1000	LHS N=500	LHS N=300	LHS N=100
Mean value	$f_1$ (Hz)	0.2321	0.2321	0.2321	0.2321	0.2321	0.2321
	$f_2$ (Hz)	0.239	0.239	0.239	0.239	0.239	0.239
	$f_3$ (Hz)	0.2515	0.2515	0.2515	0.2514	0.2516	0.2514
Standard deviation	$f_1$ (Hz)	0.005	0.005	0.0051	0.0049	0.0051	0.0049
	$f_2$ (Hz)	0.0057	0.0057	0.0057	0.0058	0.0056	0.0056
	$f_3$ (Hz)	0.0139	0.0139	0.0139	0.0139	0.014	0.0135

Table 2 Statistical moments of the first three natural frequencies for  $CV = 0.2$  and  $\rho = 0.5$

	$f_1$ (Hz)	$f_2$ (Hz)	$f_3$ (Hz)
Mean	0.232	0.239	0.251
Variance	0.005	0.006	0.014
Skewness	0.189	-0.261	0.674
Kurtosis	3.251	3.931	3.625

In Fig. 2 are shown the graphs of the probabilistic distribution of the first three natural frequencies of the building obtained considering  $\rho = 0.5$  and  $CV = 0.2$ . In the same figure it can be observed the comparison with the normal probability density functions with the same mean values and standard deviations. It is possible to note from Fig. 2 and Table 2 that the probability distributions are non-Gaussian with positive skewness and kurtosis. The possible overlapping of the natural frequencies does not influence the effectiveness of the Monte Carlo-based optimization procedure (Adhikari and Friswell 2007).

The advantage in considering the uncertainty directly on the mass distribution is that it is not necessary to make simplified hypothesis on the probability density function of the natural frequencies and their correlation as it is often done in many literature references.

#### 5.4 Optimization of the passive control system

As in this case study three uni-directional ATMDs are considered, the design variables vector (Eq. (12)) is reduced to

$$\Psi = \{k_{lx}, k_{cx}, c_{lx}, c_{cx}\} \tag{21}$$

where  $k_{lx}$  is the stiffness of the lateral ATMDs,  $k_{cx}$  is the stiffness of the central TMD,  $c_{lx}$  is the damping of the lateral ATMDs,  $c_{cx}$  is the damping of the central TMD. The subscript  $x$  specifies that all the TMDs can move along the  $x$  direction.

The upper and lower bounds to the terms of the design variables vector  $\psi_{i, \min}$  and  $\psi_{i, \max}$  are obtained with a preliminary sensitivity analysis.

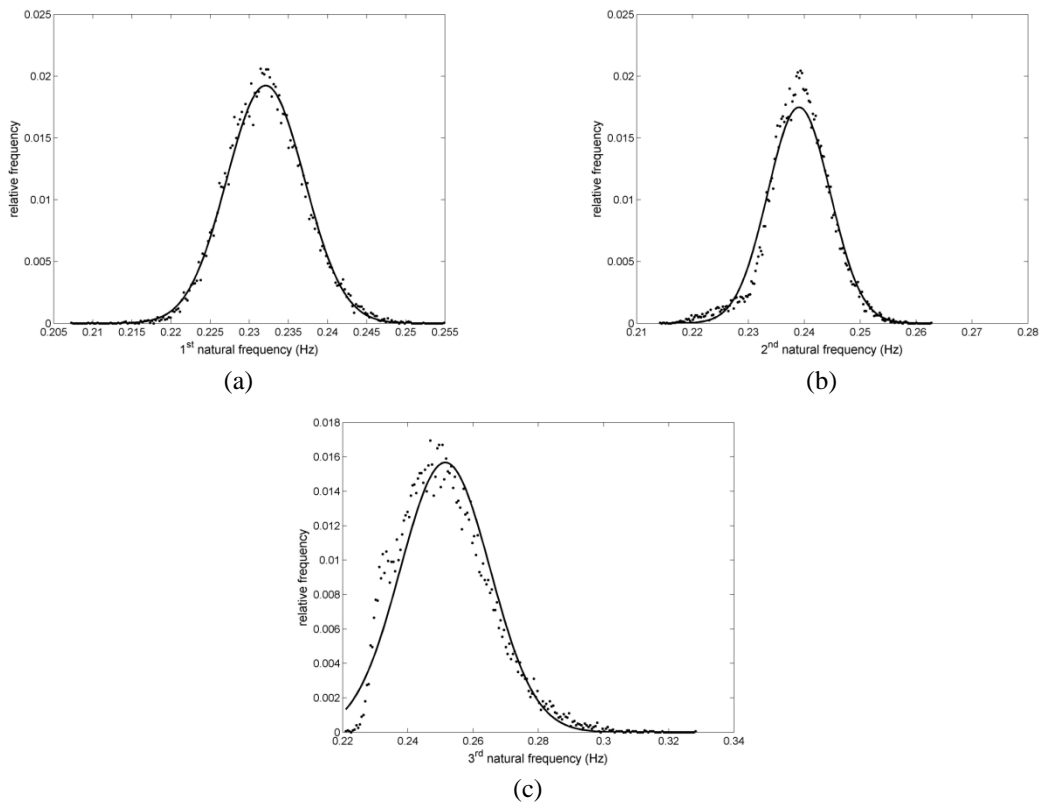


Fig. 2 Relative frequencies of the 1<sup>st</sup> (a), 2<sup>nd</sup> (b) and 3<sup>rd</sup> (c) natural frequencies compared to the corresponding normal distributions

The objective function is expressed by Eq. (13), where the sum is extended only to the alongwind and torsional components of the structural response.

The parameters of the genetic algorithm, chosen with a preliminary sensitivity analysis in order to guarantee a sufficient accuracy of the results, are reported in Table 3.

The effect of mass in modifying damping is considered in the numerical procedure. In

particular, adopting a damping ratio equal to 1% and the design (deterministic) values of the mass and stiffness matrices, the Rayleigh coefficients  $\alpha$  and  $\beta$  are computed. Then, the mass-dependent damping matrices are evaluated using the sample mass matrices and the Rayleigh coefficients  $\alpha$  and  $\beta$ . If the maximum coefficient of variation  $CV = 0.6$  and a correlation coefficient  $\rho = 0.5$  are adopted, the corresponding damping ratio varies between 0.82% and 1.23%.

In Fig. 3 is shown the relative frequencies diagram of the objective function obtained with  $CV = 0.4$  and  $\rho = 0.5$ . The vertical lines represent the interval  $\bar{F}_1 \pm \sigma_{F_1}$  where  $\bar{F}_1$  is the mean value of the objective function and  $\sigma_{F_1}$  is its standard deviation. The selected interval corresponds to the robust solutions, that lie in the neighborhood of the mean value of the distribution.

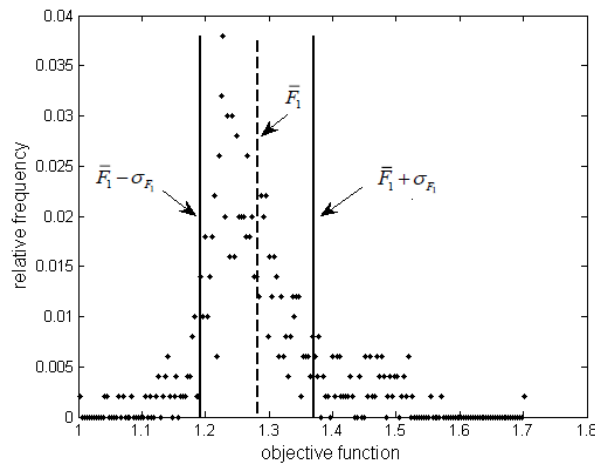


Fig. 3 Relative frequency of the objective function  $F_1(\psi)$

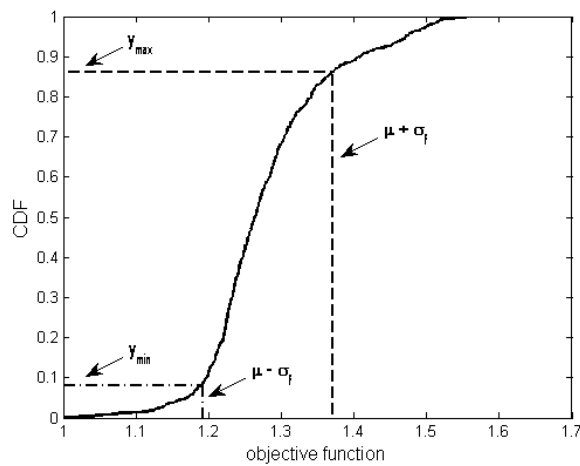


Fig. 4 Confidence interval and level

Table 3 Parameters of the genetic algorithm

PARAMETER	VALUE
Population size	30
Maximum iterations number	100
Function tolerance	$10^{-6}$
Elite count	2
Crossover fraction	0.8
Migration fraction	0.2

The choice of the amplitude of the confidence interval  $\bar{F}_1 \pm \sigma_{F_1}$  is based on a preliminary sensitivity analysis. In Fig. 4 is shown the cumulative distribution function (CDF) of the objective function obtained for  $\rho = 0.5$  and  $CV = 0.4$ . The vertical lines represent the boundaries of the confidence interval and the horizontal lines represent the corresponding probability of non exceedance. From the figure it can be inferred that the confidence level is about 80% that may be considered an acceptable compromise between the need of reducing the confidence interval and the need of having a sufficiently high confidence level. Table 4 reports the confidence intervals and levels for the different cases that have been analyzed. The confidence levels vary between 77% and 80% and the probability of non exceedance of the upper threshold of the confidence interval is greater than 86% for all the analyzed cases.

Table 4 Confidence intervals and levels for different coefficients of variation and correlation coefficients

		$\bar{F}_1 - \sigma_{F_1}$	$\bar{F}_1 + \sigma_{F_1}$	$P_{\min} (\%)$	$P_{\max} (\%)$	Confidence level (%)
$CV = 0.2$	$\rho = 0.5$	1.216	1.321	8.6	85.6	77.0
$CV = 0.4$	$\rho = 0.5$	1.192	1.371	8.0	86.2	78.2
$CV = 0.6$	$\rho = 0.5$	1.187	1.353	8.8	86.5	77.7
$CV = 0.4$	$\rho = 0$	1.193	1.381	7.6	86.4	78.8
$CV = 0.4$	$\rho = 0.5$	1.192	1.371	8.0	86.2	78.2
$CV = 0.4$	$\rho = 1$	1.210	1.377	7.8	87.8	80.0

Table 5 Statistical parameters of the *robust* optimal stiffnesses ( $\cdot 10^5$  N/m) and dampings ( $\cdot 10^4$  Ns/m) for  $\rho = 0.5$ 

	Coefficient of variation											
	0.2				0.4				0.6			
	$k_{lx}$	$k_{cx}$	$c_{lx}$	$c_{cx}$	$k_{lx}$	$k_{cx}$	$c_{lx}$	$c_{cx}$	$k_{lx}$	$k_{cx}$	$c_{lx}$	$c_{cx}$
Mean	1.013	4.350	0.684	4.288	1.169	4.489	0.849	4.362	1.937	5.446	3.531	5.621
Variance	0.039	0.022	0.061	0.164	0.339	0.408	0.547	0.974	4.004	4.545	6.425	7.214
Skewness	6.885	-0.162	2.154	0.455	4.459	-0.122	4.428	3.953	2.126	0.222	0.856	0.597
Kurtosis	55.42	1.448	12.70	3.616	25.71	44.72	24.35	22.86	7.157	4.291	1.787	2.150

In Fig. 5 are shown the relative frequencies of the design variables obtained with  $CV = 0.4$  and  $\rho = 0.5$ . In the same graph are reported the histogram corresponding to *all* the samples and the histogram corresponding to the *robust* samples. This latter are the solutions corresponding to the optimal values of the objective functions comprises in the interval  $\bar{F}_1 \pm \sigma_{F_1}$ , that are the *robust* solutions. The optimal stiffness and damping of the lateral TMDs are in general more skewed than the corresponding parameters of the central TMDs. Moreover, the optimal stiffness are less scattered than the corresponding optimal damping.

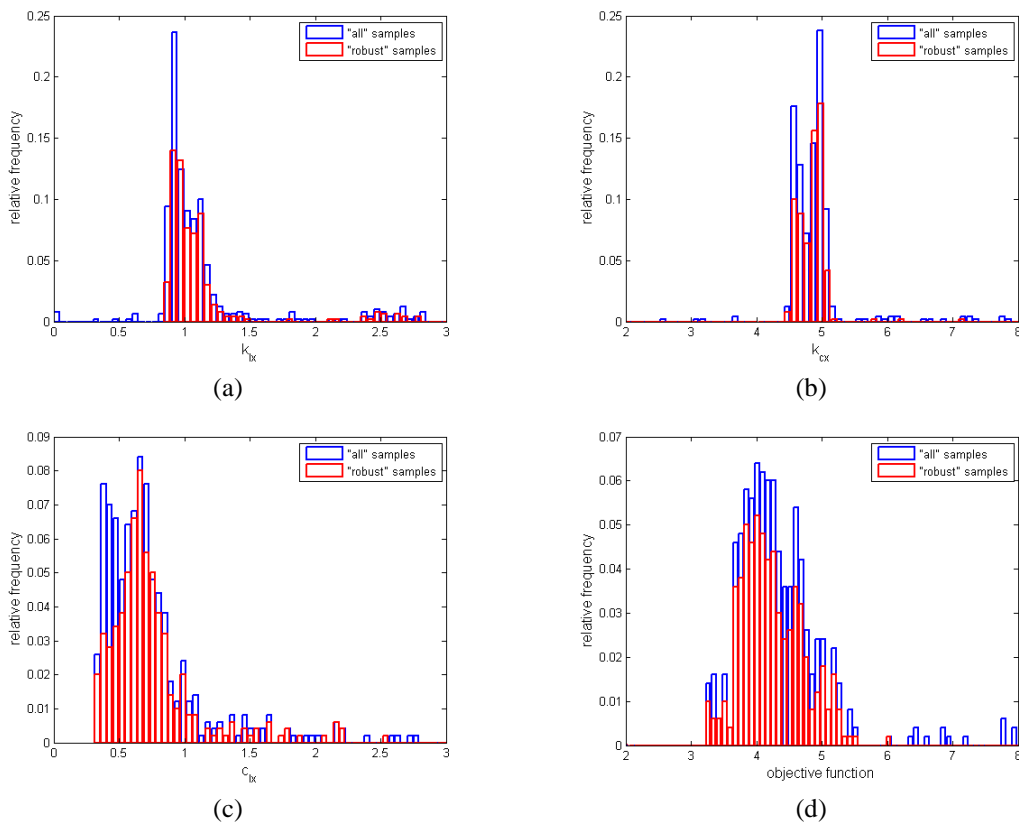


Fig. 5 Relative frequency histograms of the optimal values of the design variables: (a)  $k_{lx}$ , (b)  $k_{cx}$ , (c)  $c_{lx}$  and (d)  $c_{cx}$

In Tables 5 and 6 are summarized the statistical moments up to the 4<sup>th</sup> order of the robust optimal values of the design variables.

In Fig. 6 are shown the relative frequencies of the objective functions obtained with different values of the coefficient of variation and different values of the correlation coefficients. In the same graphs are reported the corresponding normal distributions. In Table 6 are summarized the mean values and the standard deviations of the optimal values of the objective function as a function of the coefficient of variation and the correlation coefficient. It can be observed that the

standard deviation of the objective function increases with the coefficient of variation.

Table 6 Statistical parameters of the *robust* optimal stiffnesses ( $\cdot 10^5$  N/m) and dampings ( $\cdot 10^4$  Ns/m) for  $CV = 0.4$

	Correlation coefficient											
	0				0.5				1			
	$k_{lx}$	$k_{cx}$	$c_{lx}$	$c_{cx}$	$k_{lx}$	$k_{cx}$	$c_{lx}$	$c_{cx}$	$k_{lx}$	$k_{cx}$	$c_{lx}$	$c_{cx}$
Mean	1.200	4.392	0.936	4.523	1.169	4.489	0.849	4.362	1.059	4.919	0.791	4.228
Variance	0.496	0.464	0.739	1.076	0.339	0.408	0.547	0.974	0.029	0.334	0.327	0.697
Skewness	3.632	4.591	3.333	3.979	4.459	-0.122	4.428	3.953	0.027	7.017	6.265	4.783
Kurtosis	17.15	40.37	15.07	20.74	25.71	44.72	24.35	22.86	9.016	53.48	46.14	32.86

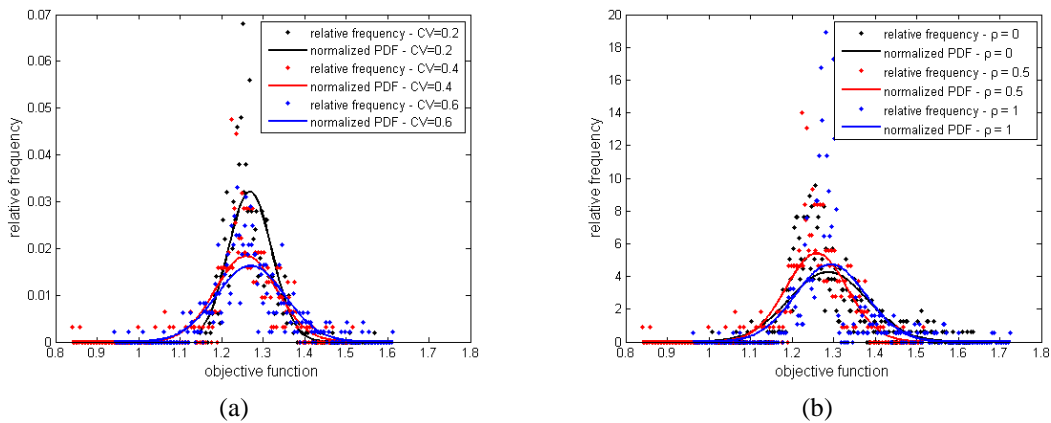


Fig. 6 Relative frequencies of the design variables obtained for different coefficients of variation (a) and different correlation coefficients (b)

In Fig. 7 are reported the relative frequency histograms of the objective function obtained with two different sets of data. The blue histogram is obtained using *all* the sample sets of the optimal design variables and the deterministic mass matrix. The red histogram is obtained using the *robust* sample sets of the optimal design variables (those corresponding to the solutions lying in the range  $\bar{F}_1 \pm \sigma_{F_1}$ , Fig. 3), and the deterministic mass matrix. The deterministic components of the mass matrix are the “design values”, corresponding to the 95<sup>th</sup> percentile of the mass distribution. The corresponding deterministic optimal value of the objective function is  $F_{det}$ . Fig. 7 shows that all the values obtained with the optimal design variables with reference to the deterministic system are higher than the value  $F_{det}$ . Moreover, using the robust optimal solutions the objective function, that is related to the structural response, does not exceed the value of about 1.5 and all the higher structural responses are avoided.

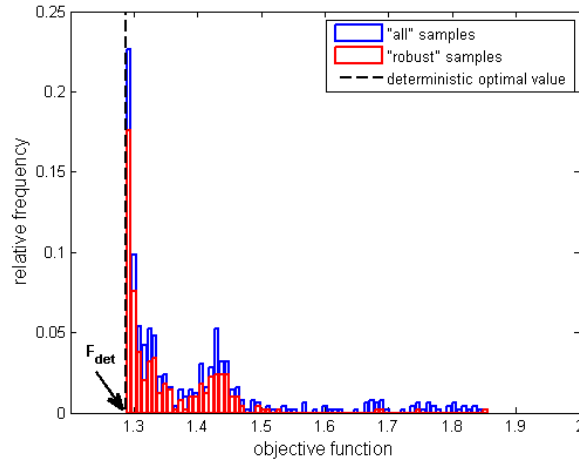


Fig. 7 Relative frequency histograms of the objective function obtained with reference to the “deterministic system”

### 5.5 Optimization of the hybrid control system

The second part of the optimization procedure is aimed at finding the optimal weight matrices  $\mathbf{R}$  and  $\mathbf{Q}$  of the control force and state vectors in the LQR performance index.

In this specific example, the coefficient  $\varphi_1$  that appears in the definition of matrix  $\mathbf{R}$  (Eq. (14)), is assumed equal to 20 and  $\mathbf{I}_1$  has dimensions (3 x 3), being 3 the degrees of freedom of the control system.

The matrix  $\mathbf{Q}$  that weights the states of the system (Eq. (15)) has dimensions (42 x 42), being (18+3) the degrees of freedom of the controlled system. In particular, based on a preliminary sensitivity analysis, a weight coefficient equal to 1 is assigned to the displacements and the velocities of the structure, a weight coefficient equal to 0 is assigned to the velocities of the actuators and a weight coefficient equal to  $10^2$  is assigned to the structural rotations in order to increase the importance of the torsional response reduction.

Therefore, the design variables are the weight coefficients of the displacements of the central ( $\varphi_2$ ) and lateral ( $\varphi_3$ ) ATMDs

$$\Psi = \{\varphi_2, \varphi_3\} \quad (22)$$

The upper and lower bounds to the terms of the design variables vector  $\psi_{i,\min}$  and  $\psi_{i,\max}$  are obtained with a preliminary sensitivity analysis. The upper bound to the stroke of each ATMD is  $q_{TMD,\max} = 2$  m while the upper bound to the control force is  $u_{\max} = 1000$  KN. The objective function is expressed by Eq. (17) where the sum is extended only to the alongwind and torsional responses.

In Fig. 7 is shown the relative frequency of the objective function obtained with  $CV = 0.4$  and  $\rho = 0.5$ . The vertical lines delimit the interval  $\bar{F}_2 \pm \sigma_{F_2}$  where  $\bar{F}_2$  is the mean value of the

objective function and  $\sigma_{F_2}$  is its standard deviation. The selected interval corresponds to the robust solutions, that lie in the neighborhood of the mean value of the distribution. In Fig. 8 are plotted the relative frequencies of the design variables for  $CV = 0.4$  and  $\rho = 0.5$  obtained using *all* the samples and the *robust* samples. The variability of the optimal values of  $\phi_2$  and  $\phi_3$  is small and their relative frequencies are slightly skewed to the right.

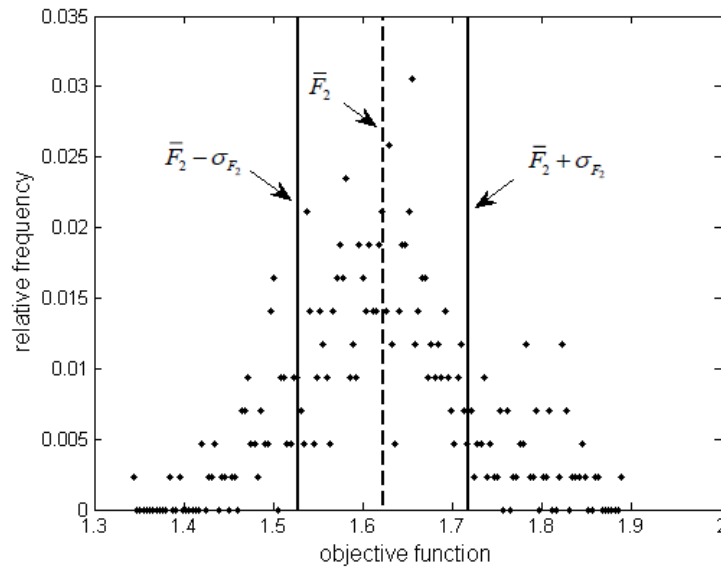


Fig. 8 Relative frequency of the objective function  $F_2(\Phi)$

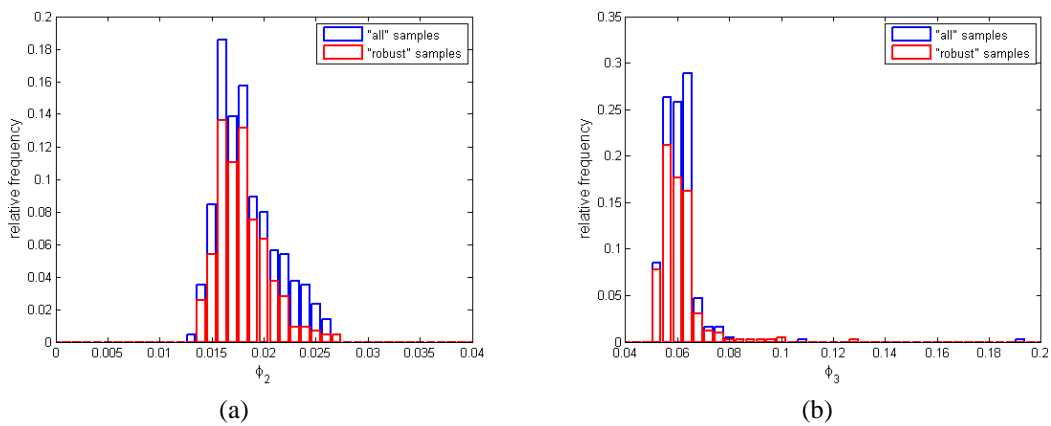


Fig. 9 Relative frequency histograms of the optimal values of the design variables : (a)  $\phi_2$ , (b)  $\phi_3$

Table 7 Mean value and standard deviation of the optimal value of the objective function

		Mean	Standard deviation
$CV = 0.2$	$\rho = 0.5$	1.268	0.053
$CV = 0.4$	$\rho = 0.5$	1.281	0.089
$CV = 0.6$	$\rho = 0.5$	1.270	0.083
$CV = 0.4$	$\rho = 0$	1.287	0.094
$CV = 0.4$	$\rho = 0.5$	1.281	0.089
$CV = 0.4$	$\rho = 1$	1.293	0.084

## 6. Conclusions

In this paper is studied the influence of the uncertain mass distribution over the floors on the choice of the optimal parameters of a hybrid control system for tall buildings subjected to wind load. An optimization procedure is developed for the robust design of a hybrid control system that is based on an enhanced Monte Carlo simulation technique and a genetic algorithm. The procedure allows to find the probability distribution of the objective function and the design variables. The robust optimal sets of the design variables are those corresponding to the optimal values of the objective function lying in the neighborhood of the mean value of the distribution. Several numerical analyses are carried out varying the parameters influencing the distribution of the floors' masses, like the coefficient of variation of the distribution and the correlation between the floors' masses showing the significant influence of the coefficient of variation on the variance of the objective function's distribution. The numerical analyses showed that using the robust optimal solutions and the design value of the mass matrix, the control system is efficient in mitigating the structural response and almost insensitive with respect to the mass variations.

## References

- Adhikari, S. and Friswell, M. I. (2007), "Random matrix eigenvalue problems in structural dynamics", *Int. J. Numer. Meth. Eng.*, **69**, 562-591.
- Beyer, H.G. and Sendhoff, B. (2007), "Robust optimization - a comprehensive survey", *Comput. Method. Appl. M.*, **196**(33-34), 3190-3218.
- Casciati, F., Rodellar, J. and Yildirim, U. (2012), "Active and semi-active control of structures-theory and applications: a review of recent advances", *J. Intel. Mat. Syst. Str.*, **23**(11), 1181-1195.
- Casciati S. (2008), "Stiffness identification and damage localization via differential evolution algorithms", *Struct. Health Monit.*, **15**(3), 436-449.
- Chakraborty, S. and Roy, B.K. (2011), "Reliability based optimum design of Tuned Mass Damper in seismic vibration control of structures with bounded uncertain parameters", *Probabilist Eng. Mech.*, **26**(2), 215-221.
- Chen, S.H., Song, M. and Chen, Y.D. (2007), "Robustness analysis of responses of vibration control structures with uncertain parameters using interval algorithm", *Struct. Saf.*, **29**(2), 94-111.
- Cluni, F., Gusella, V. and Ubertini, F. (2007), "A parametric investigation of wind-induced cable fatigue", *Eng. Struct.*, **29**(11), 3094-3105.

- Conn, A.R. and Le Digabel, S. (2013), "Use of quadratic models with mesh-adaptive direct search for constrained black box optimization", *Optim. Method Softw.*, **28**(1), 139-158.
- Doltsinis, I. and Kang, Z. (2004), "Robust design of structures using optimization methods", *Comput. Method. Appl. M.*, **193**(23-26), 2221-2237.
- Gioffrè, M., Gusella, V., Materazzi, A.L. and Venanzi, I. (2004), "Removable guyed mast for mobile phone networks: Wind load modeling and structural response", *J. Wind Eng. Ind. Aerod.*, **92**(6), 463-475.
- Goldberg, D.E. (1989), *Genetic Algorithms in Search, Optimization and Machine Learning*, Addison Wesley Publishing Company.
- Grooteman, F. (2011), "An adaptive directional importance sampling method for structural reliability", *Probabilist Eng. Mech.*, **26**(2), 134-141.
- Hoang, N., Fujino, Y. and Warnitchai, P. (2008), "Optimal tuned mass damper for seismic applications and practical design formulas", *Eng. Struct.*, **30**(3), 707-715.
- Huntington, D.E. and Lyrintzis, C.S. (1998), "Improvements to and limitations of Latin hypercube sampling", *Probabilist Eng. Mech.*, **13**(4), 245-253.
- Iman, R.L. (2008), *Latin Hypercube Sampling*, Encyclopedia of Quantitative Risk Analysis and Assessment.
- Jensen, H.A. (2006), "Structural optimization of non-linear systems under stochastic excitation", *Probabilist Eng. Mech.*, **21**(4), 397-409.
- Katafygiotis, L.S. and Wang, J. (2009), "Reliability analysis of wind-excited structures using domain decomposition method and line sampling", *Struct. Eng. Mech.*, **32**(1), 37-53.
- Lee, K.H. and Park, G.J. (2001), "Robust optimization considering tolerances of design variables", *Comput. Struct.*, **79**(1), 77-86.
- Li, H.S. and Au, S.K. (2010), "Design optimization using subset simulation algorithm", *Struct. Saf.*, **32**(6), 384-392.
- Marano, G.C. and Greco, R. (2009), "Robust optimum design of tuned mass dampers for high-rise buildings under moderate earthquakes", *Struct. Des. Tall Spec.*, **18**(8), 823-838.
- Marano, G.C., Greco, R. and Sgobba, S. (2010), "A comparison between different robust optimum design approaches: application to tuned mass dampers", *Probabilist Eng. Mech.*, **25**, 108-118.
- Moreno, C.P. and Thomson, P. (2010), "Design of an optimal tuned mass damper for a system with parametric uncertainty", *Ann Oper Res.*, **181**(1), 783-793.
- Olsson, A., Sandberg, G. and Dahlblom, O. (2003), "On Latin hypercube sampling for structural reliability analysis", *Struct. Saf.*, **25**(1), 47-68.
- Pascual, B. and Adhikari, S. (2012), "Combined parametric-nonparametric uncertainty quantification using random matrix theory and polynomial chaos expansion", *Comput. Struct.*, **112-113**, 364-379.
- Pradlwarter, H.J., Schuëller, G.I., Koutsourelakis, P.S. and Charmpis, D.C. (2007), "Application of line sampling simulation method to reliability benchmark problems", *Struct. Saf.*, **29**(3), 208-221.
- Schuëller, G.I. and Jensen, H.A. (2008), "Computational methods in optimization considering uncertainties - an overview", *Comput. Methods Appl. M.*, **198**(1), 2-13.
- Song, S., Lu, Z. and Qiao, H. (2009), "Subset simulation for structural reliability sensitivity analysis", *Reliab. Eng. Syst. Safe.*, **94**(2), 658-665.
- Venanzi, I., Ubertini, F. and Materazzi, A.L. (2013), "Optimal design of an array of active tuned mass dampers for wind-exposed high-rise buildings", *Struct. Health Monit.*, **20**(6), 903-917.
- Venanzi, I. and Materazzi, A.L. (2012), "Acrosswind aeroelastic response of square tall buildings: a semi-analytical approach based of wind tunnel tests on rigid models", *Wind Struct.*, **15**(6), 495-508.
- Venanzi, I. and Materazzi, A.L. (2007), "Multi-objective optimization of wind-excited structures", *Eng. Struct.*, **99**(6), 983-990.
- Warburton, G.B. (1982), "Optimum absorber parameters for various combination of response and excitation parameters", *Earthq. Eng. Struct. D.*, **10**(3), 381-401.
- Zhang, H. (2012), "Interval importance sampling method for finite element-based structural reliability assessment under parameter uncertainties", *Struct. Saf.*, **38**, 1-10.